Kinetics and Mechanism of Oxygen Transfer in the Reaction of *p*-Cyano-*N*,*N*-dimethylaniline *N*-Oxide with Metalloporphyrin Salts. 7.[1,2] Oxygen Atom Transfer to and from (*meso*-Tetrakis(pentafluorophenyl)porphinato)iron(III) Chloride

Dražen Ostovič, Carolyn B. Knobler, and Thomas C. Bruice*

Contribution from the Department of Chemistry, University of California at Santa Barbara, Santa Barbara, California 93106. *Received November 3, 1986*

Abstract: The decomposition of *p*-cyano-*N*,*N*-dimethylaniline *N*-oxide (NO) in the presence of (*meso*-tetrakis(pentafluorophenyl)porphinato)iron(III) chloride ($(F_{20}TPP)Fe^{III}Cl$) provides *p*-cyano-*N*,*N*-dimethylaniline (DA) in 32 ± 3%, *p*-cyano-*N*-methylaniline (MA) in 50 ± 5%, 4-cyano-7-(dimethylamino)-2-benzofuranone-3-spiro-2′-cyano-5′-(dimethylamino)cyclopentadiene (BF) in 16 ± 2%, and formaldehyde in 30 ± 3% yield based upon $[NO]_i$. Material balance may be accounted for in all components. Appearance of products is first order in both NO and $(F_{20}TPP)Fe^{III}Cl$, and the second-order rate constant for the reaction has been determined to be $(2.0 \pm 0.5) \times 10^2$ M^{-1} s^{-1}. The observation that the formation of products DA, MA, and BF is associated with the same rate constant establishes the commitment step to be the bimolecular reaction of NO with $(F_{20}TPP)Fe^{III}Cl$. It is proposed that this reaction directly yields DA and the iron(IV)–oxo porphyrin π-cation radical ($(^{+\bullet}F_{20}TPP)Fe^{IV}O$). That the formation of $(^{+\bullet}F_{20}TPP)Fe^{IV}O$ + DA is rate controlling is substantiated by use of the reagents 2,4,6-tri-*tert*-butylphenol (TBPH), *N*,*N*-dimethylaniline (DMA), and *N*,*N*-dimethyltoluidine (DMT) as traps for the $(^{+\bullet}F_{20}TPP)Fe^{IV}O$ species. The rates of oxidation of these trapping agents are independent of their concentration, and the rate constants calculated for the appearances of their oxidation products correspond to the turnover rate constant for the reaction of NO with $(F_{20}TPP)Fe^{III}Cl$ in the absence of trapping agents. Formation of the products MA and BF must then be attributed to the rapid oxidation of DA by $(^{+\bullet}F_{20}TPP)Fe^{IV}O$. The formation of MA occurs by the oxidative demethylation of DA, and formation of BF is logically accounted for by the hydroxylation of DA to yield 2-hydroxy-4-cyano-*N*,*N*-dimethylaniline (DMP) which, on further stepwise oxidation, provides BF (much as in the stepwise $1e^-$ oxidation of *p*-cresol to yield Pumerer's ketone). Increase in the concentrations of DMA and DMT results in exponential increase in the percentage yield of DA and decrease in the percentage yield of MA. In each case the asymptotic percentage yields of 68 ± 7% DA and 17 ± 2% MA are approached. The percentage yield of BF (17 ± 2%) is not changed by the presence of DMA or DMT at various concentrations or by their absence. These results show that a substantial portion of the immediate products DA and $(^{+\bullet}F_{20}TPP)Fe^{IV}O$ reacts in a solvent-caged $/(^{+\bullet}F_{20}TPP)Fe^{IV}O{\cdot}DA/$ pair prior to their diffusion apart. Once free from the caged pair, the $(^{+\bullet}F_{20}TPP)Fe^{IV}O$ species oxidizes the traps DMA and DMT in preference to DA. The asymptotic yield of MA represents the percentage yield of MA obtained by oxidation of DA within the solvent caged pair. Since the percentage yield of BF is not influenced by the presence of DMA or DMT, all hydroxylation of DA must occur within the $/(^{+\bullet}F_{20}TPP)Fe^{IV}O{\cdot}DA/$ species. By this reasoning, both the caged oxidative demethylation and hydroxylation of DA occur in ~17% yields. Thus, within the $/(^{+\bullet}F_{20}TPP)Fe^{IV}O{\cdot}DA/$ caged pair there is no discrimination between hydroxylation of the aromatic ring of DA and its oxidative demethylation. When TBPH is employed as trap the asymptotic yields of DA and MA have the same values as obtained with DMA and DMT. This provides additional support for the formation of MA in 17% yield by oxidation of DA within the solvent-caged pair. In the presence of TBPH the formation of BF is not observed. Aromatic ring hydroxylation of DA provides DMP which is converted to BF only after further oxidation by $(^{+\bullet}F_{20}TPP)Fe^{IV}O$ which has diffused from the solvent cage. The inability to detect BF in the presence of TBPH is probably best attributed to the observed trapping of all free $(^{+\bullet}F_{20}TPP)Fe^{IV}O$ by TBPH.

In previous publications we have described the dynamics of the reactions of *p*-cyano-*N*,*N*-dimethylaniline *N*-oxide (NO) with variously ligated (*meso*-tetraphenylporphinato)manganese(III) compounds (axial ligands being F^-, Cl^-, Br^-, I^-, OCN^-, and imidazole)[1] and with variously phenyl-substituted (*meso*-tetraphenylporphinato)iron(III) salts in the presence and absence of various alkenes.[2] In the reaction of NO with an Mn(III) or Fe(III) tetraphenylporphyrin an oxygen-transfer reaction occurs (eq 1)

$$(Porph)Fe^{III}X + NO \rightleftarrows ((Porph)Fe^{III}ON)X \rightarrow DA + ((^{+\bullet}Porph)Fe^{IV}O)X \quad (1)$$

to provide *p*-cyano-*N*,*N*-dimethylaniline (DA) and a higher valent iron–oxo porphyrin. The rate-determining step involves, in all cases, the oxygen-transfer reaction, so the structure of the iron–oxo porphyrin species cannot be determined from these experiments. From spectroelectrochemical studies the iron–oxo porphyrin species, $2e^-$ oxidized above the iron(III) state, has been identified as an iron(IV)–oxo porphyrin π-cation radical ($(^{+\bullet}Porph)Fe^{IV}O$).[3] In non-rate-determining reactions DA is oxidized to a series of identified products by $(^{+\bullet}Porph)Fe^{IV}O$. In the presence of added oxidizable substrates (alkenes, 2,4,6-tri-*tert*-butylphenol, etc.) there is a competition for $(^{+\bullet}Porph)Fe^{IV}O$ by the added substrate and by DA and its oxidation products (eq 2). From the changes in

$$((^{+\bullet}Porph)Fe^{IV}O)Cl \xrightarrow[\text{alkene}]{p\text{-}CNPhNMe_2} \begin{matrix}(Porph)Fe^{III}Cl + CH_2O + p\text{-}CNPhNH(Me)\\ (Porph)Fe^{III}Cl + \text{expoxide}\end{matrix} \quad (2)$$

the dynamics of products formation which accompany changes in the structure of the porphyrin moiety there has been discerned

(1) (a) Powell, M. F.; Pai, E. F.; Bruice, T. C. *J. Am. Chem. Soc.* **1984**, *106*, 3277. (b) Wong, W.-H.; Ostovic, D.; Bruice, T. C., submitted for publication in *J. Am. Chem. Soc.*

(2) (a) Shannon, P.; Bruice, T. C. *J. Am. Chem. Soc.* **1981**, *103*, 4500. (b) Nee, M. W.; Bruice, T. C. *Ibid.* **1982**, *104*, 6123. (c) Dicken, C. M.; Lu, F.-L.; Nee, M. W.; Bruice, T. C. *Ibid.* **1985**, *107*, 5776. (d) Dicken, C. M.; Woon, T.-C.; Bruice, T. C. *Ibid.* **1986**, *108*, 1636. (e) Woon, T.-C.; Dicken, C. M.; Bruice, T. C. *Ibid.*, in press. (f) Bruice, T. C.; Dicken, C. M.; Balasubramanian, P. N.; Woon, T.-C.; Lu, F.-L., submitted for publication in *J. Am. Chem. Soc.*

(3) (a) Lee, W. A.; Calderwood, T. S.; Bruice, T. C. *Proc. Natl. Acad. Sci. U.S.A.* **1985**, *82*, 4301. (b) Calderwood, T. S.; Lee, W. A.; Bruice, T. C. *J. Am. Chem. Soc.* **1985**, *107*, 8272. (c) Calderwood, T. S.; Bruice, T. C. *Inorg. Chem.* **1986**, *25*, 3722.

0002-7863/87/1509-3444$01.50/0

a number of structure–reactivity relationships which relate to the efficiency of epoxidation vs. demethylation and $1e^-$ oxidations and to the rates of oxygen transfer from NO to (Porph)$Fe^{III}X$ species.

We report herein an investigation of the reaction of NO with (*meso*-tetrakis(pentafluorophenyl)porphinato)iron(III) chloride ($(F_{20}TPP)Fe^{III}Cl$). The salt $(F_{20}TPP)Fe^{III}Cl$ represents the most electron-deficient iron(III) porphyrin which has been examined. Our findings include the observations that a large portion of DA oxidation occurs prior to the diffusion apart of DA and $((^{+\bullet}F_{20}TPP)Fe^{IV}O)Cl$. Also, we find that within the solvent cage $/((^{+\bullet}F_{20}TPP)Fe^{IV}O)Cl{\cdot}DA/$ the two reactions of hydroxylation of the aromatic ring of DA (a feature not previously observed in the reaction of NO with other substituted tetraphenylporphyrins) and demethylation of DA compete equally. After dissociation of $/((^{+\bullet}F_{20}TPP)Fe^{IV}O)Cl{\cdot}DA/$ the bimolecular reaction of the components $((^{+\bullet}F_{20}TPP)Fe^{IV}O)Cl$ + DA results only in the demethylation of DA.

Experimental Section

Materials. The solvent CH_2Cl_2 used throughout this study was of the highest purity, and its preparation has been described previously as Grade A.[2c] (*meso*-Tetrakis(pentafluorophenyl)porphinato)iron(III) chloride ($(F_{20}TPP)Fe^{III}Cl$) was purchased from Aldrich and Porphyrin Products. *cis*-Cyclooctene (Aldrich) was distilled under N_2 atmosphere. 2,4,6-Tri-*tert*-butylphenol (TBPH) was purchased from Aldrich, and its purification has been described previously.[2c] *N,N*-Dimethylaniline (DMA) and *N,N*-dimethyl-*p*-toluidine (DMT) (Aldrich) were purified by vacuum distillation. *p*-Cyano-*N,N*-dimethylaniline *N*-oxide (NO) was prepared by the method of Craig and Purushothaman[4] and was recrystallized from acetone/petroleum ether under dry N_2 atmosphere. 4-Cyano-7-(dimethylamino)-2-benzofuranone-3-spiro-2'-cyano-5'-(dimethylamino)-cyclopentadiene (BF) was prepared and isolated in the following way: NO (0.5 g, 3.1 mmol) was dissolved in CH_2Cl_2 (20 mL), and a solution of $(F_{20}TPP)Fe^{III}Cl$ (5 mg, 4.7 nmol) in CH_2Cl_2 (2 mL) was added under anaerobic conditions. The reaction was complete after 10 min at room temperature. The volume of the reaction mixture was reduced to ~5 mL, and the products were separated by column chromatography on silica (flash, 200–400 mesh). DA and MA were eluted with 3:1 hexane/ethyl acetate. The solvent was then changed to pure ethyl acetate. The yellow fraction was collected and recrystallized from ethyl acetate/hexane to yield 20 mg of pure BF product: mp 207–208 °C. ^1H NMR δ 2.82 (s, 6 H), 3.16 (s, 6 H), 5.00 (d, J = 3.3 Hz, 1 H), 6.63 (d, J = 8.9 Hz, 1 H), 7.24 (d, J = 8.9 Hz, 1 H), 7.42 (d, J = 3.3 Hz, 1 H); IR ($CHCl_3$) 2942 w, 2887 w, 2808 w, 2226 w, 2198 w, 1806 s, 1615 vs, 1597 s, 1532 vs, 1422 vs. 1374 w, 1253 w, 1130 m, 1033 m, 997 m, 885 w cm^{-1}; mass spectrum (70 ev), m/e (relative intensity) 320.4 (100) M^+; UV–vis λ_{max} (ϵ, M^{-1} cm^{-1}) 397 (1.07×10^4), 299 (1.78×10^4).

Details of the procedures and techniques for the determination of the X-ray structure of BF are provided in the supplementary material. The structure of BF is provided in the Results section.

Analysis for formaldehyde was carried out by a modification of the standard method of Nash.[5] The reaction mixture (1 mL) was shaken well with H_2O (3 mL) in a screw-capped, sealed vial. A 1-mL aliquot of the aqueous phase was reacted with 3 mL of Nash "B" reagent. The reaction was quantitatively complete in 2 h, as judged by the increase in the absorbance at 412 nm where only the product, 3,5-diacetyl-1,4-dihydropyridine, absorbs. The reaction follows the first-order rate law ($t_{1/2}$ = 11.4 min at 25 °C), and the rate is independent of $[CH_2O]$. A standard curve was prepared in an analogous way by using CH_2O solutions of known concentration, giving $[CH_2O] = (A_{412}/601) \pm 3\%$ when using a 1-cm path length cuvette.

HPLC and GC methods of product analysis have been described previously.[2c]

Electrochemical studies were carried out as previously described.[3]

Kinetics of Reaction of $(F_{20}TPP)Fe^{III}Cl$ with NO (CH_2Cl_2 Solvent at 25 ± 0.1 °C) in the Presence and Absence of Added Substrates. Under an N_2 atmosphere, solutions of the iron(III) porphyrin chloride and NO were placed in the separate chambers of a number of Thunberg cuvettes. The cuvettes were sealed and removed from the N_2 atmosphere box, and kinetic runs were initiated by mixing after thermal equilibration of the solutions. The reaction progress was monitored spectrophotometrically between 280 and 385 nm for at least seven half-lives. For those reactions involving the addition of the substrates, TBPH, DMA, DMT, and cyclooctene, the substrates were included with the iron(III) porphyrin chloride in the bottom port of the cuvette.

(4) Craig, J. C.; Purushothman, K. K. *J. Org. Chem.* **1970**, *35*, 1721.
(5) Nash, T. *Biochem. J.* **1953**, *55*, 416.

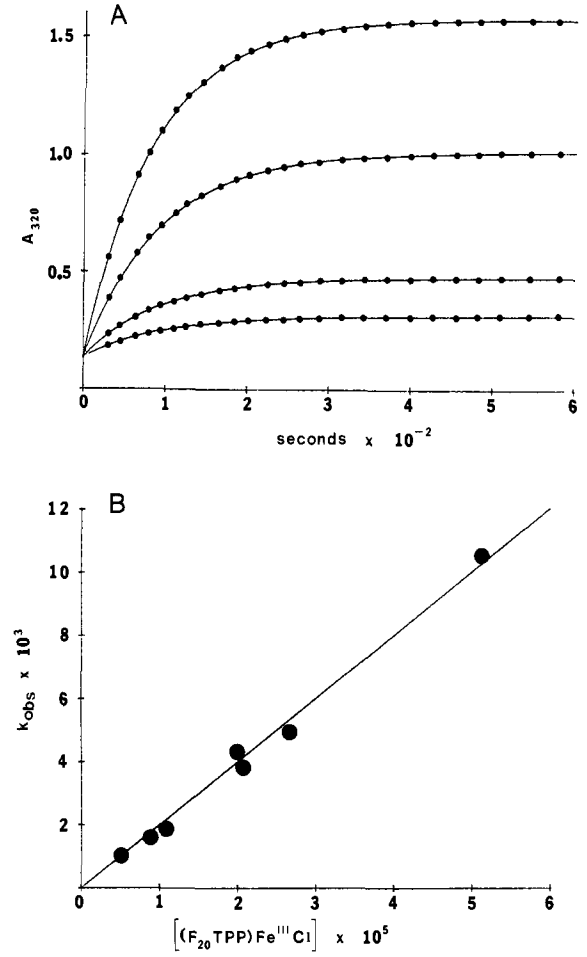

Figure 1. (A) Plots of A_{320} vs. time for the $(F_{20}TPP)Fe^{III}Cl$-catalyzed decomposition of *p*-cyano-*N,N*-dimethylaniline *N*-oxide (NO) ($[(F_{20}TPP)Fe^{III}Cl]_i = 5.14 \times 10^{-5}$ M, $[NO]_i$ varied from 5.05×10^{-4} to 5.05×10^{-3} M) showing that the initial rates are dependent on $[NO]_i$ but that k_{obsd} is independent of $[NO]_i$. The points are experimental, and the lines are computer generated by use of the first-order rate law. (B) Plot of k_{obsd} vs. $[(F_{20}TPP)Fe^{III}Cl]_i$ showing the linear dependence of k_{obsd} on $[(F_{20}TPP)Fe^{III}Cl]$. The slope yields an apparent second-order rate constant of 2.0×10^2 M^{-1} s^{-1}.

The individual rates of formation of DA and MA were followed by HPLC. Solutions of NO (1.07×10^{-3} M, 1 mL) were sealed in gas-tight nitrogen-filled vials and thermostated at 25 °C when a solution of $(F_{20}TPP)Fe^{III}Cl$ (1.14×10^{-4} M, 0.1 mL) was injected with a gas-tight syringe. After given time intervals, a vial was selected, and a 50-μL aliquot was withdrawn and applied to the HPLC column. The concentrations of DA and MA at various extents of reaction were determined from standard curves. The rate of formation of BF was conveniently monitored spectrophotometrically at 385 nm where DA and MA show no absorption. We were not able to follow the time course for the appearance of CH_2O, due to the fact that the reaction is too fast. With $[(F_{20}TPP)Fe^{III}Cl] = 1 \times 10^{-5}$ M, $t_{1/2}$ for the reaction (~5 min) is comparable to the time required to quench the reaction in order to determine the concentration of CH_2O.

Results

Reaction of $(F_{20}TPP)Fe^{III}Cl$ with NO yields *p*-cyano-*N,N*-dimethylaniline (DA), *p*-cyano-*N*-methylaniline (MA), 4-cyano-7-(dimethylamino)-2-benzofuranone-3-spiro-2'-cyano-5'-(dimethylamino)cyclopentadiene (BF), and CH_2O. The time course for the appearance of these products can be monitored either collectively by UV–vis spectrophotometry between 280 and 320 nm or selectively by HPLC. HPLC analysis of the reaction mixture at 280 and 320 nm shows that the yields of DA and MA are 32 ± 3% and 50 ± 5%, respectively. The yield of BF cannot be determined accurately by HPLC analysis (elution time 46 min) due to its partial decomposition on the column; however, BF shows a long wavelength absorbance with maximum at 397 nm. The

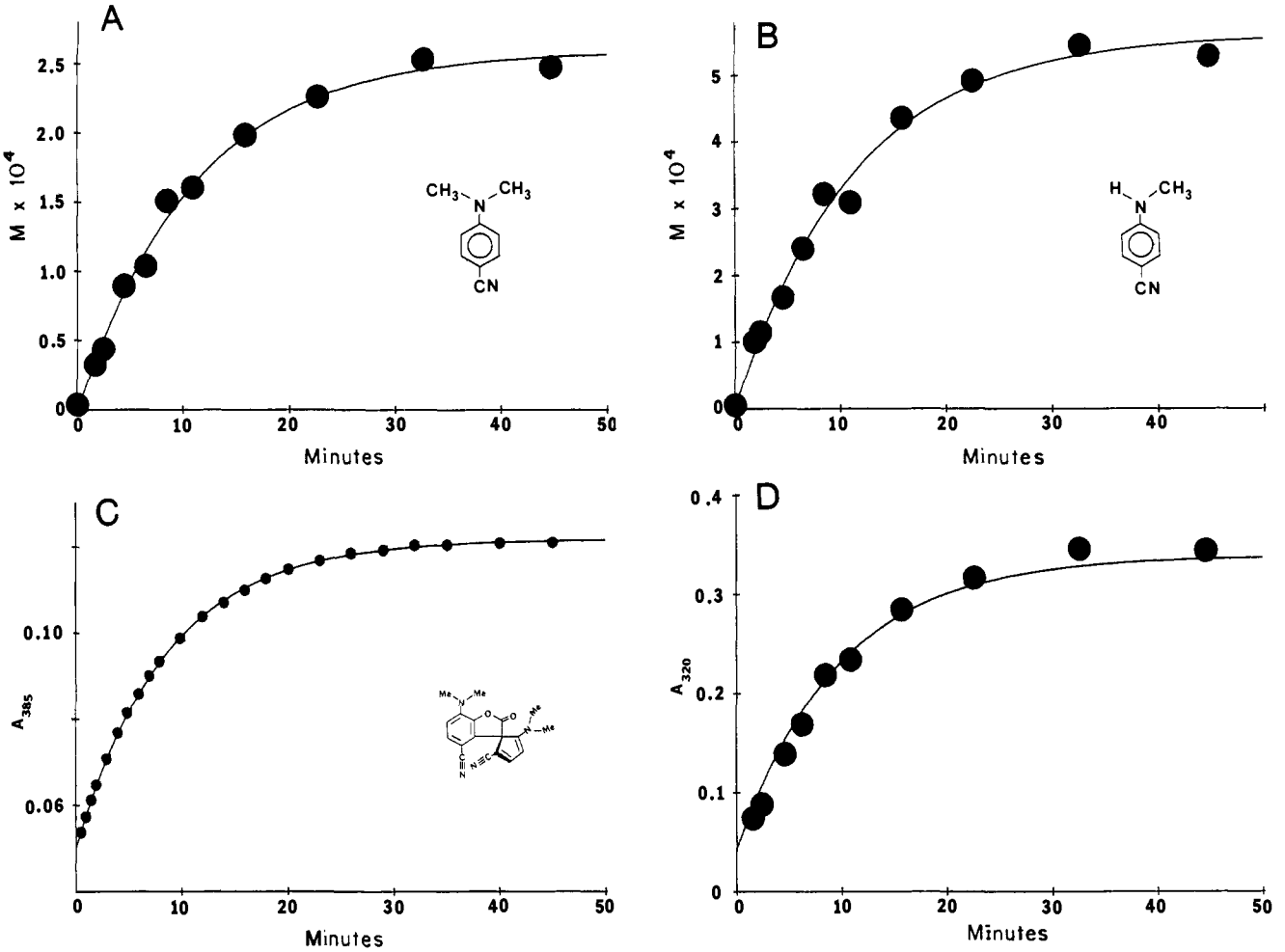

Figure 2. Time courses for the products formed in the $(F_{20}TPP)Fe^{III}Cl$ (1.04×10^{-5} M) catalyzed decomposition of *p*-cyano-*N*,*N*-dimethylaniline *N*-oxide (9.7×10^{-4} M): (A) *p*-cyano-*N*,*N*-dimethylaniline (determined by HPLC); (B) *p*-cyano-*N*-methylaniline (determined by HPLC); (C) 4-cyano-7-(dimethylamino)-2-benzofuranone-3-spiro-2′-cyano-5′-(dimethylamino)cyclopentadiene (determined from the change in absorbance at 385 nm); and (D) the first-order computer-fitted line of the spectral trace at 320 nm is superimposed to the points representing the experimentally determined summations of the concentrations of products A–C (expressed as absorbance at 320 nm) at various extents of the reaction.

yield of BF was calculated from ΔA_{385} on completion of the reaction. A wavelength of 385 nm was used because it corresponds

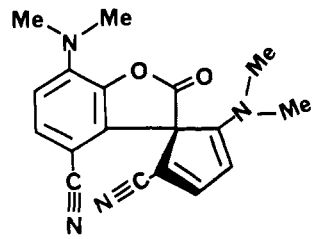

BF

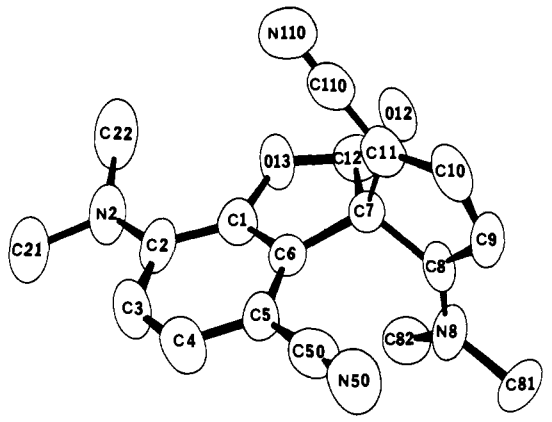

BF

to a minimal absorbance of $(F_{20}TPP)Fe^{III}Cl$. Though the extinction coefficients of $(F_{20}TPP)Fe^{III}Cl$ (ϵ 4.43×10^4 M^{-1} cm^{-1}) and BF (ϵ 1.03×10^4 M^{-1} cm^{-1}) are comparable at 385 nm, the latter is present in much higher concentrations at completion of the reactions. The yield of BF calculated in this manner was 16 ± 2%, based on the NO. Together with the yields of DA and MA (32% and 50%, respectively) 98% of the nitrogen originated in NO is accounted for in products. The yield of CH_2O (30 ± 3%) was found to be independent of the concentrations of all reactants. Formaldehyde formation occurs on oxidation of DA → MA so that ~20% CH_2O remains unaccounted for. If it is assumed that the missing CH_2O has been further oxidized to HCO_2H, then 102% of the oxygen originated in NO is accounted for. Thus, material balance in all components is accounted for.

Under the pseudo-first-order conditions of $[NO]_i \gg [(F_{20}TPP)Fe^{III}Cl]_i$ the appearance of products (320 nm) follows the first-order rate law with continual turnover of the iron(III) porphyrin catalyst (Figure 1a). The oberved pseudo-first-order rate constant (k_{obsd}) is linearly proportional to the concentration of $(F_{20}TPP)Fe^{III}Cl$ (Figure 1B). Though, for 10–200 turnovers of the catalyst, initial rates are linearly dependent upon $[NO]_i$, the values of k_{obsd} are not. These results establish that, with the concentrations of reactants employed, the catalyst is not saturated with NO. The apparent second-order rate constant ($k_{obsd}/[(F_{20}TPP)Fe^{III}Cl]$) has been determined as $(2.0 \pm 0.5) \times 10^2$ M^{-1} s^{-1} from the slope of the line of Figure 1B.

The rates of formation of each product were determined as described in the Experimental Section. The results are shown in Figure 2A–C. Concentrations of DA, MA, and BF products formed with time were converted to absorbances at 320 nm by using appropriate extinction coefficients, and these absorbances

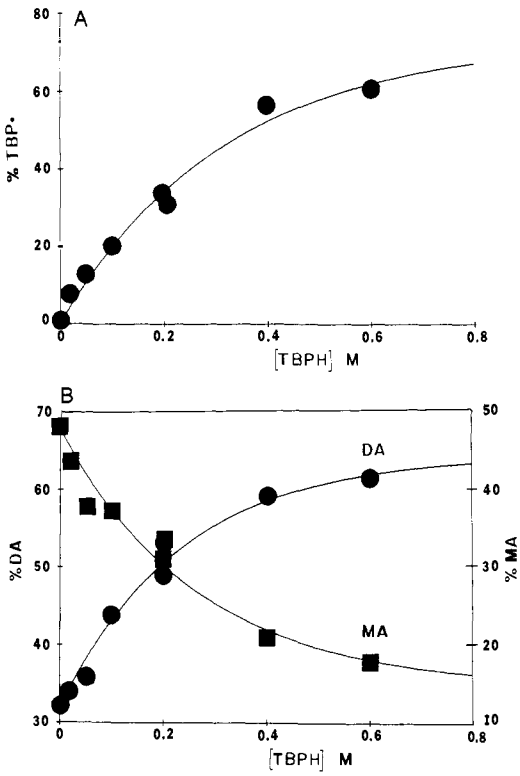

Figure 3. Plots of the variation in the percentage yields (based on the concentration of *p*-cyano-*N*,*N*-dimethylaniline *N*-oxide) of (A) 2,4,6-tri-*tert*-butylphenoxyl radical (TBP•) and (B) *p*-cyano-*N*,*N*-dimethylaniline (DA) (●) and *p*-cyano-*N*-methylaniline (MA) (■) as a function of the increase in the concentration of 2,4,6-tri-*tert*-butylphenol (TBPH). The points are experimental, and the lines represent single-exponential best fit.

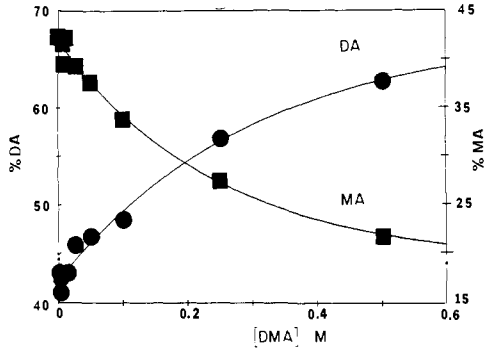

Figure 4. Plots of the variation in the percentage yields of *p*-cyano-*N*,*N*-dimethylaniline (DA) (●) and *p*-cyano-*N*-methylaniline (MA) (■) (based on the initial concentration of *p*-cyano-*N*,*N*-dimethylaniline *N*-oxide (NO)) as a function of the increase in the initial concentration of *N*,*N*-dimethylaniline (DMA). The points are experimentally determined values, and the lines represent the best single-exponential fits.

were added. The results are shown in Figure 2D. In Figure 2D the points are the experimentally determined summation of the concentrations of DA, MA, and BF (expressed as absorbance at 320 nm) while the line is that obtained by following the appearance of all products spectrophotometrically at 320 nm. Examination of Figure 2 shows (i) that the concentrations of various products at different extents of the reaction, when expressed as absorbances and summed, mimic very well the spectral trace at 320 nm and (ii) that all products are formed at the identical rate, within the experimental error. The latter finding indicates that all products are formed after the rate-determining step of oxygen transfer from NO to $(F_{20}TPP)Fe^{III}Cl$.

The rate constant for the transfer of the oxene equivalent from NO to $(F_{20}TPP)Fe^{III}Cl$ was independently determined by trapping the higher valent iron–oxo porphyrin species with 2,4,6-tri-*tert*-butylphenol (TBPH).[6] In separate experiments it was shown that

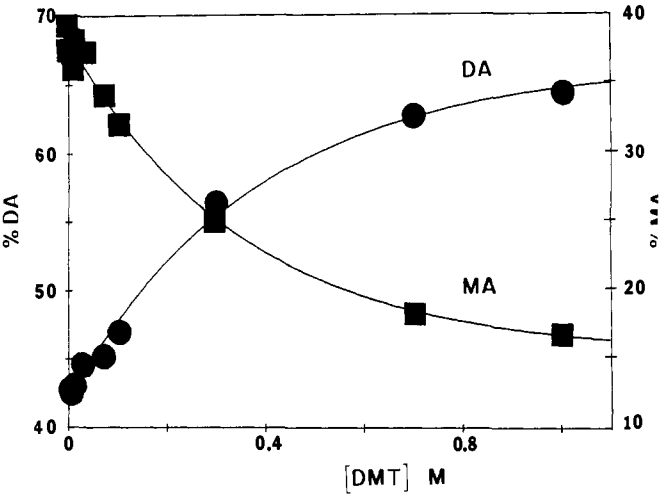

Figure 5. Plots of the variation in the percentage yields of *p*-cyano-*N*,*N*-dimethylaniline (DA) (●) and *p*-cyano-*N*-methylaniline (MA) (■) (based on the initial concentration of *p*-cyano-*N*,*N*-dimethylaniline N-oxide (NO)) as a function of the increase in the initial concentration of *N*,*N*-dimethyltoluidine (DMT). The points are experimentally determined values, and the lines represent the best single-exponential fits.

TBPH does not react with $(F_{20}TPP)Fe^{III}Cl$ or NO under the conditions of the experiments. The reaction was monitored by following the formation of TBP• at 630 nm (ϵ 400 M^{-1} cm^{-1} in CH_2Cl_2). When the absorbance allowed (i.e., at low [TBPH], 1-mm cells), the reactions were simultaneously monitored at 320 and 385 nm. The increases of A_{630}, A_{320}, and A_{385} followed the first-order rate law to >90% of completion of the reaction. The apparent first-order rate constant for the appearance of TBP• is independent of [TBPH], establishing that TBP• is formed after the rate-limiting step. The observed first-order rate constant divided by $[(F_{20}TPP)Fe^{III}Cl]$ yields $(1.6 \pm 0.2) \times 10^2$ M^{-1} s^{-1} as the rate constant for the bimolecular oxygen atom transfer from NO to $(F_{20}TPP)Fe^{III}Cl$, eq 3. This value is in good agreement

$$NO + (F_{20}TPP)Fe^{III}Cl \rightarrow DA + ((^{+\bullet}F_{20}TPP)Fe^{IV}O)Cl$$

$$((^{+\bullet}F_{20}TPP)Fe^{IV}O)Cl + 2TBPH \rightarrow (F_{20}TPP)Fe^{III}Cl + 2TBP^{\bullet} + H_2O \quad (3)$$

with $k_{obsd}/[(F_{20}TPP)Fe^{III}Cl] = (2.0 \pm 0.5) \times 10^2$ M^{-1} s^{-1}, determined from the increase in absorbance at 320 and 385 nm with time for the reactions in which NO and $(F_{20}TPP)Fe^{III}Cl$ were the only reactants. The yield of TBP•, with increase in $[TBPH]_i$, asymptotically approaches the value of 73 ± 4%, and similarly the yields of DA and MA at the same time approach 65 ± 2% and 15 ± 3%, respectively. At the high concentrations of TBPH used in trapping experiments the yield of BF cannot be determined spectroscopically due to the overlap of its spectrum with the spectra of TBPH and TBP•. HPLC analysis indicates that the yield of BF decreases with increase in [TBPH]; at [TBPH] = 0.1 M, no BF can be detected. The results are summarized in Figure 3. These results indicate that part of the $((^{+\bullet}F_{20}TPP)Fe^{IV}O)Cl$ species is consumed by reaction with DA within the solvent cage immediately after oxygen transfer from NO to $(F_{20}TPP)Fe^{III}Cl$.

The electron-rich tertiary amines, *N*,*N*-dimethylaniline (DMA) and *N*,*N*-dimethyl-*p*-toluidine (DMT), were added to the reaction mixture in order to compete with DA in the demethylation reaction. Addition of these amines to the reaction mixture does not change the rate constant for $(F_{20}TPP)Fe^{III}Cl$ catalyst turnover in its reaction with NO. These reactions were monitored spectrophotometrically between 320 and 385 nm depending on the concentration of the added amine. The average observed rate constants divided by $[(F_{20}TPP)Fe^{III}Cl]$ were $(1.4 \pm 0.2) \times 10^2$ M^{-1} s^{-1} when DMA was added and $(2.1 \pm 0.5) \times 10^{-2}$ M^{-1} s^{-1}

(6) Traylor, T. G.; Lee, W. A.; Stynes, D. V. *J. Am. Chem. Soc.* **1984**, *106*, 755.

Table I. Asymptotic Percentage Yields of DA, MA, and BF Obtained in the Presence of Various Traps

trapping agent	percentage yield[a] DA	MA	BF
TBPH[b]	65	15	0
DMA	68	19	16
DMT	67	15	18

[a] The yields have ±10% uncertainty due to the experimental error. [b] The yield of TBP• approaches 73% based on $[NO]_i$.

Table II. Effect of *cis*-Cyclooctene Concentration on the Percentage Yields (Based on $[NO]_i = 1.0 \times 10^{-3}$ M) of DA, MA, BF, and Cyclooctene Oxide[a]

[alkene], M	percentage yield DA	MA	BF	epoxide	k_2, M^{-1} s^{-1}
0	32.4	45.1	16.6	0	254
0.2	33.9	40.8	17.5	4.3	237
1.0	37.8	37.6	18.6	6.3	210

[a] Concentration of $(F_{20}TPP)Fe^{III}Cl$ catalyst = 2.0×10^{-5} M; $k_{obsd}/[(F_{20}TPP)Fe^{III}Cl]_i = k_2$.

when DMT was added. The only detected oxidation products of DMA and DMT were the corresponding monomethylanilines MMA and MMT, respectively (eq 4). The yield of BF was

$$((^{+\bullet}F_{20}TPP)Fe^{IV}O)Cl + DMA \rightarrow (F_{20}TPP)Fe^{III}Cl + MMA + CH_2O$$

$$((^{+\bullet}F_{20}TPP)Fe^{IV}O)Cl + DMT \rightarrow (F_{20}TPP)Fe^{III}Cl + MMT + CH_2O \quad (4)$$

constant (17 ± 2%) regardless of the concentration of the added amine. The yields of DA and MA were determined by using HPLC, and they showed systematic changes as a function of the concentrations of added tertiary amine. The results are shown in Figures 4 and 5. Inspection of Figures 4 and 5 shows that DMA and DMT cannot quantitatively trap the higher valent oxo species formed during the reaction of NO and $(F_{20}TPP)Fe^{III}Cl$. In the reactions where DMA was added, the yields of DA and MA approached asymptotically 68% and 19% with increase in $[DMA]_i$. Similarly, in the reactions where DMT was added as a trapping reagent, the yields of DA and MA approach asymptotically 67% and 15%, respectively. The yields of DA, MA, and BF in the presence of various trapping reagents are summarized in Table I.

The oxidation of *cis*-cyclooctene by NO (1.0×10^{-3} M) in the presence of $(F_{20}TPP)Fe^{III}Cl$ (2.0×10^{-5} M) was determined by capillary GC. *cis*-Cyclooctene was chosen on the basis that it is fairly reactive toward epoxidations by higher valent iron–oxo porphyrin species and it is well separated by GC from its epoxide (epoxide retention time 6.3 min vs. cyclooctene at 3.2 and CH_2Cl_2 at 1.4 min). The rate of $(F_{20}TPP)Fe^{III}Cl$ catalyst turnover with NO is not affected by addition of *cis*-cyclooctene up to 1 M ($k_{obsd}/[(F_{20}TPP)Fe^{III}Cl] = (2.2 \pm 0.2) \times 10^2$ M^{-1} s^{-1}). The yields of various products are summarized in Table II. From the data in Table II, it follows that cyclooctene is not able to compete successfully with DA for $((^{+\bullet}F_{20}TPP)Fe^{IV}O)Cl$. This will be shown to be due, in part, to much of the DA oxidation occurring within a solvent cage of DA and the oxidant.

Discussion

In the presence of (*meso*-tetrakis(pentafluorophenyl)porphinato)iron(III) chloride ($(F_{20}TPP)Fe^{III}Cl$) in dichloromethane solvent at 25 °C, *p*-cyano-*N*,*N*-dimethylaniline *N*-oxide (NO) is decomposed to *p*-cyano-*N*,*N*-dimethylaniline (DA), 32%; *p*-cyano-*N*-methylaniline (MA), 50%; 4-cyano-7-(dimethylamino)-2-benzofuranone-3-spiro-2′-cyano-5′-(dimethylamino)-cyclopentadiene (BF), 16%; and formaldehyde, 30%.

2-Hydroxy-4-cyano-*N*,*N*-dimethylaniline (DMP) is a required intermediate for the formation of BF. The formation of DMP on reaction of $(F_{20}TPP)Fe^{III}Cl$ with NO offers the first example of aromatic ring hydroxylation with higher valent iron–oxo species when NO is used as the oxygen-transferring reagent. It has previously been reported that anisole is hydroxylated by iodosylbenzene in the presence of $(F_{20}TPP)Fe^{III}Cl$.[7] It is well appreciated that phenols are easily oxidized to the corresponding dienone radicals by $1e^-$ oxidizing agents such as ferricyanide. The resulting dienone radicals undergo coupling reactions, of which the formation of Pumerer's ketone has received considerable attention.[8]

Scheme I

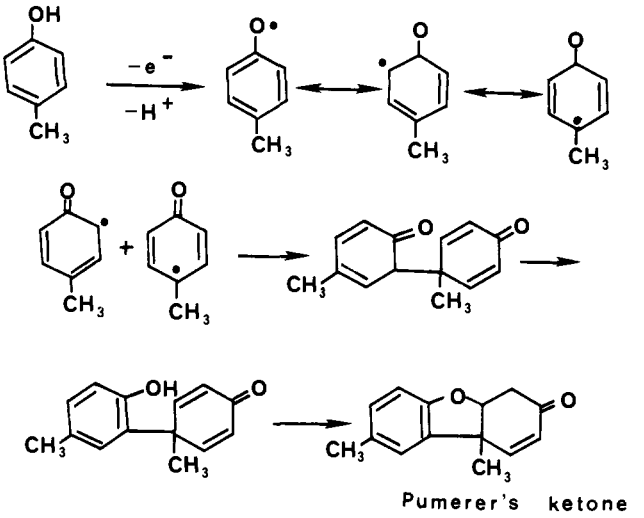

A proposed mechanism for the formation of Pumerer's ketone is provided in Scheme I. A similar type of chemistry is proposed to occur during the formation of BF. The plausible mechanism is depicted in Scheme II. The hydroxylation of DA ortho to the dimethylamino group is followed by 1e–oxidation to yield the corresponding dienone radical DMP•. Coupling of two dienone radicals followed by enolization and addition of hydroxyl group across carbonyl yields hemiketal (HK), which can oxidatively rearrange to BF.

In the reaction of NO with $(F_{20}TPP)Fe^{III}Cl$, the iron(III) porphyrin is not consumed as judged by the spectrum of the reaction mixtures at completion of reaction. From turnover kinetics, under the condition of $[NO]_i \gg [(F_{20}TPP)Fe^{III}Cl]_i$, the reaction has been shown to be first order in both NO and $(F_{20}TPP)Fe^{III}Cl$, and the second-order rate constant (k_2) equals (2.0 ± 0.5) × 10^2 M^{-1} s^{-1}. The rate constants for the formation of the products DA, MA, and BF are, within the experimental error, identical with that for the overall turnover reaction. Since NO yields DA on oxygen transfer to iron(III) porphyrin and both MA and BF arise from competitive pathways of DA oxidation, the finding that their rates of formation are identical shows that oxygen transfer from NO to $(F_{20}TPP)Fe^{III}Cl$ is rate limiting.

Rate-limiting oxygen transfer from NO to a number of iron(III) porphyrins in CH_2Cl_2 solvent [i.e., (*meso*-tetraphenylporphinato)iron(III) chloride ($(TPP)Fe^{III}Cl$), (*meso*-tetrakis(2,6-dimethylphenyl)porphinato)iron(III) chloride ($(Me_8TPP)Fe^{III}Cl$), and (*meso*-tetrakis(2,6-dichlorophenyl)porphinato)iron(III) chloride ($(Cl_8TPP)Fe^{III}Cl$), as well as (*meso*-tetrakis(2,6-dimethylphenyl)porphinato)manganese(III) ligated to imidazole] has been established,[1,2] by trapping the intermediate iron(IV)–oxo porphyrin π-cation radicals with 2,4,6-tri-*tert*-butylphenol (TBPH). The oxygen transfer is established, by this procedure, to be rate limiting (eq 3) when the rate constant for the formation of the TBPH $1e^-$ oxidation product (TBP•) is independent of [TBPH], and is the same as the rate constant for catalyst turnover. Trapping of all iron(IV)–oxo porphyrin π-cation radical produces DA and TBP• in 100% yield based upon $[NO]_i$ as shown in eq 3. In the present study we find that the rate

(7) Chang, C. K.; Ebina, F. *J. Chem. Soc., Chem. Commun.* **1981**, 778.
(8) (a) Barton, D. H. R.; Deflorin, A. M.; Edwards, O. E. *J. Chem. Soc.* **1956**, 530. (b) Arkley, V.; Dean, F. M.; Robertson, A.; Sidisunthorn, P. *J. Chem. Soc.* **1956**, 2322. (c) Bruice, T. C. *J. Org. Chem.* **1958**, *23*, 246.

Scheme II

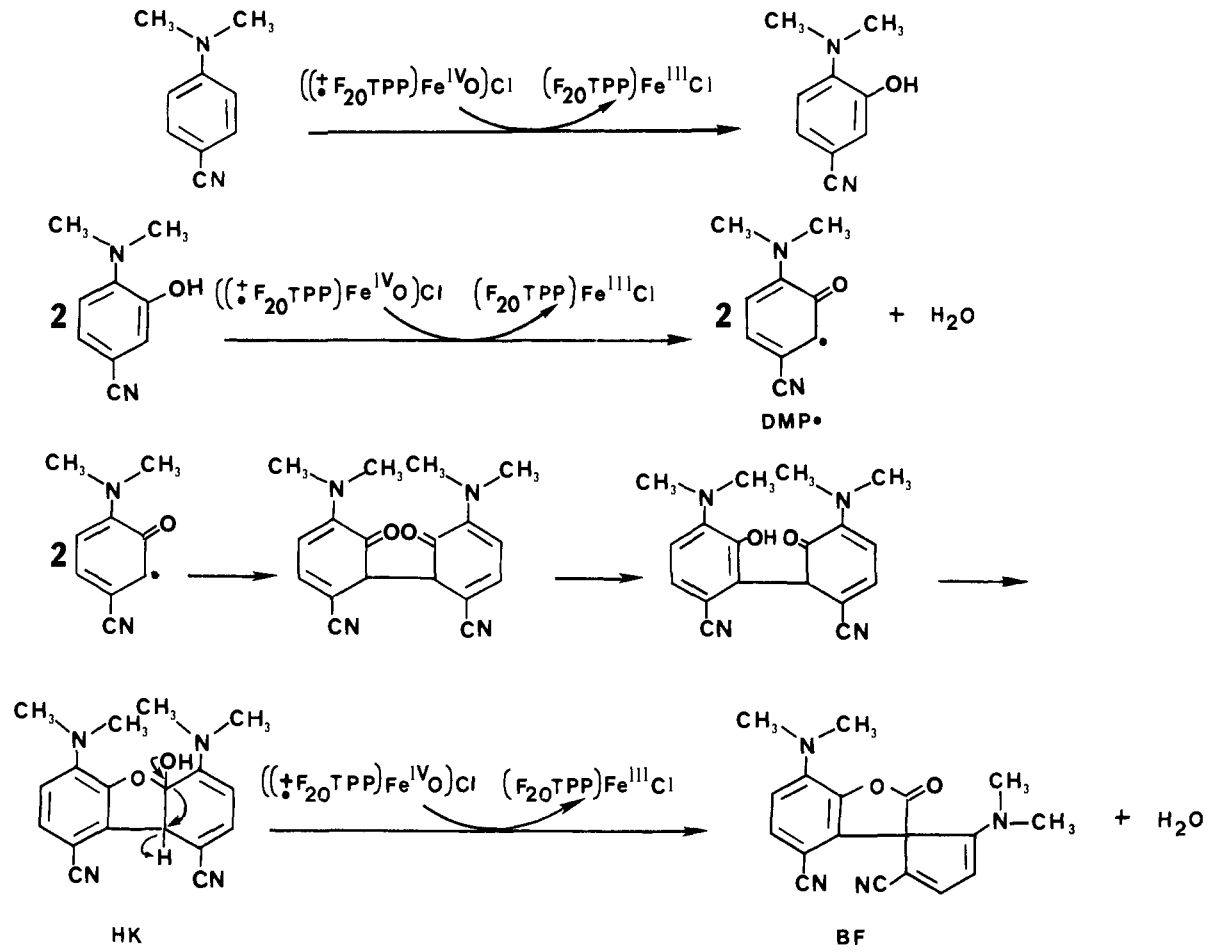

constant for formation of TBP• from TBPH is independent of the latter's concentration and equal to that for catalyst turnover in the absence of TBPH. We also find, however, that the yields of neither DA nor TBP• approach 100%. Thus, though the rate constant for TBP• formation remains constant with increase in $[TBPH]_i$, the percentage yields of DA and TBP• increase with increase in TBPH to asymptotic values of 65% and 73%, respectively. At the same time the yield of the DA oxidation product MA decreases with increase in $[TBPH]_i$ to an asymptotic value of 15% (Figure 3A). On increase in $[TBPH]_i$, the percentage yield of BF rapidly decreases to zero. *p*-Cyano-*N*,*N*-dimethylaniline (DA) and $((^{+\bullet}F_{20}TPP)Fe^{IV}O)Cl$ are formed on oxygen transfer from NO to iron(III) porphyrin whereas *p*-cyano-*N*-methylaniline (MA) is produced from DA by consumption of 1 equiv of $((^{+\bullet}F_{20}TPP)Fe^{IV}O)Cl$, and BF must arise from DA by the consumption of 2 equiv of $((^{+\bullet}F_{20}TPP)Fe^{IV}O)Cl$. At all concentrations of TBPH, the combined yields of DA and MA are constant at 81 ± 8%. Without the presence of TBPH there is obtained material balance in both the oxygen and nitrogen derived from NO, but at high $[TBPH]_i$ there is an imbalance in nitrogen (based upon the yields of DA, MA, and BF) of ~19%. This 19% imbalance in nitrogen is equivalent, within the experimental error, to the percentage yield of BF obtained in the absence of the trapping agent. It would appear that TBPH or its $1e^-$ oxidation product, TBP•, either is capable of trapping an intermediate which leads to BF (probably the radical DMP•, Scheme II), or is successful in trapping the $(^{+\bullet}F_{20}TPP)Fe^{IV}O)Cl$ intermediate.

The compounds *N*,*N*-dimethylaniline (DMA) and *N*,*N*-dimethyltoluidine (DMT) have also been employed as trapping agents. The addition of either DMA or DMT has no effect on the rate constant for the reaction of NO with $(F_{20}TPP)Fe^{III}Cl$. With increase in either $[DMA]_i$ or $[DMT]_i$, the yields of DA and MA asymptotically approach the limiting values of 68 ± 1% and 17 ± 2%, respectively. These yields are comparable to the limiting yields obtained on adding increasing concentrations of TBPH (Table I). Most important, however, is the finding that the yield of BF (17 ± 2%) is unaffected by addition of DMA or DMT and that material balance is obtained in both nitrogen and oxygen in the presence of these agents. These results may be discussed in the frame of Scheme III.

Scheme III assumes that $(F_{20}TPP)Fe^{III}Cl$ + NO is in equilibrium with the complex $(F_{20}TPP)Fe^{III}(NO)Cl$[9] and that intracomplex oxygen transfer to provide the solvent-caged intimate pair $/((^{+\bullet}F_{20}TPP)Fe^{IV}O)Cl{\cdot}DA/$ is rate limiting. Oxidation of DA may occur within the caged intimate pair to yield either MA plus CH_2O or to provide the aminophenol DMP. Once the solvent-caged intimate pair dissociates, the free $((^{+\bullet}F_{20}TPP)Fe^{IV}O)Cl$ species then (i) oxidatively demethylates DA to yield MA and CH_2O, (ii) oxidizes CH_2O to HCO_2H, (iii) participates in the oxidation of DMP which results in the formation of BF, (iv) oxidizes TBPH to form TBP• radical, and (v) oxidatively demethylates DMA and DMT to provide the corresponding monomethylanilines plus CH_2O.

The asymptotic yields of products obtained for high concentrations of trapping agents are useful in separating the extents of reactions which occur in and out of the solvent-caged pair of $(F_{20}TPP)Fe^{IV}O$ + DA. At high concentrations of the trapping agents TBPH, DMA, and DMT, the percentage yield of MA must represent the percent of DA which has undergone oxidation to MA within the $/((^{+\bullet}F_{20}TPP)Fe^{IV}O)Cl{\cdot}DA/$ complex. At high

(9) The equilibrium constants for complexation of the $[(F_{20}TPP)Fe^{III}]^+$ moiety with the nonreacting 4-picoline *N*-oxide (PNO) to provide $(F_{20}TPP)Fe^{III}(PNO)^+$ (K_1) and $(F_{20}TPP)Fe^{III}(PNO)_2^+$ (β_2) were determined[2c] to be 3.0×10^2 and 1.5×10^5, respectively. If these constants were assumed as those for the complexing of NO, the iron(III) porphyrin catalyst would, at initiation of the kinetic runs, be ~55% saturated by NO under the experimental conditions of this study. This cannot be the case, since partial saturation would result in deviation from the observed first-order dependence of the reaction on $[NO]_i$. As shown with $(Cl_8TPP)Fe^{III}Cl$,[2d] equilibrium constants for the complexing of PNO are not useful in the prediction of the complexation of *N*,*N*-dimethylaniline *N*-oxides.

Scheme III

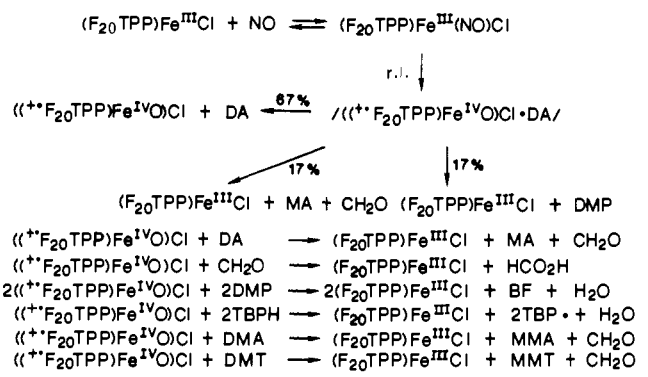

Scheme IV

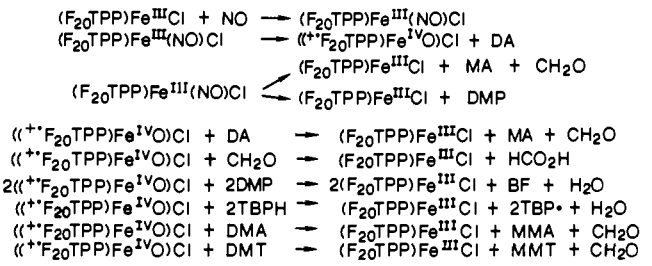

concentrations of DMA and DMT, the percentage yields of MA and BF equal the percentage of oxidation of DA to MA and DMP within the /(($^{+\bullet}F_{20}$TPP)Fe^{IV}O)Cl·DA/ complex while the percentage yield of DA represents that fraction of /(($^{+\bullet}F_{20}$TPP)Fe^{IV}O)Cl·DA/ which dissociates without undergoing an intracomplex redox reaction. By this reasoning 17% of DA undergoes oxidation to MA and 17% of DA undergoes oxidation to DMP within the solvent-caged intimate pair. About 67% of the initially formed /(($^{+\bullet}F_{20}$TPP)Fe^{IV}O)Cl·DA/ dissociates to its components.

The trap TBPH differs from DMA and DMT in that its radical product of $1e^-$ oxidation is stable, while the radical cation $1e^-$ oxidation products of DMA and DMT are unstable due to their rearrangement to a carbon radical by loss of a proton. Both DMA and DMT are unable to compete with either the formation of DMP, within the solvent-caged /(($^{+\bullet}F_{20}$TPP)Fe^{IV}O)Cl)·DA/ species, or the oxidation of DMP by free (($^{+\bullet}F_{20}$TPP)Fe^{IV}O)Cl to yield BF. Since the presence of TBPH above 0.1 M results in the absence of BF as a product but the summed yields of DA and MA are constant (the latter also being the case in the presence of DMA and DMT) regardless of the concentration of the trapping agent, it follows that TBPH does not compete with the formation of DMP by hydroxylation of DA within the /(($^{+\bullet}F_{20}$TPP)Fe^{IV}O)Cl·DA/ complex. Also, since BF is not formed in the presence of TBPH, it is clear that the oxidation of DMP by free (($^{+\bullet}F_{20}$TPP)Fe^{IV}O)Cl cannot compete with the oxidation of TBPH.

The $1e^-$ oxidation potentials for the formation of chloro-ligated iron(III) porphyrin π-cation radical species are the same as the $1e^-$ oxidation potentials for the formation of the corresponding iron(IV)–oxo porphyrin π-–cation radicals.[3a] A comparison of the $E_{1/2}$ values for the formation of chloro iron(III) porphyrin π-cation radicals is then equivalent to the comparison of the potentials of iron(IV)–oxo porphyrin π-cation radical species. The $E_{1/2}$ values of interest (CH_2Cl_2 solvent with $(n\text{-}C_4H_9)_4N^+ClO_4^-$, V vs. SCE) are ($Me_8$TPP)$Fe^{III}$Cl, +1.51; (TPP)$Fe^{III}$Cl, +1.55; ($Cl_8$TPP)$Fe^{III}$Cl, +1.77;[3a] and ($F_{20}$TPP)$Fe^{III}$Cl, +1.84 (this study). The species (($^{+\bullet}F_{20}$TPP)Fe^{IV}O)Cl is the better oxidant by 70–330 mV. This explains why the oxidation of DA within the solvent caged /(($^{+\bullet}F_{20}$TPP)Fe^{IV}O)Cl·DA/ species occurred in the same time scale as diffusion apart for this intimate pair. Rates of diffusion apart of solvent-caged species in organic solvents range from 10^7 to 10^{12} s^{-1}.[10] The ratio of MA to DMP formed by DA oxidation within the solvent-caged species is ~1:1, thus indicating the high reactivity and lack of selectivity of ($^{+\bullet}F_{20}$TPP)Fe^{IV}O.

Evidence exists for DA oxidation within a solvent-caged species for the reaction (*meso*-tetrakis(2,6-dimethylphenyl)porphinato)manganese(III) chloride ((Me_8TPP)Mn^{III}Cl) with NO in the presence of imidazole.[2b] With $[TBPH]_i$ as a trapping reagent at 0.028–0.28 M, the yields of DA and TBP• were 72 ± 5%, and the only product of the oxidative degradation of DA was MA, which was obtained in 28 ± 2% yield.[1b] This result certainly indicates that about 25–30% of the oxidation of DA occurs within a solvent-caged intimate pair. Evidence is available which may be interpreted to indicate that oxidation within a solvent-caged species occurs on reaction of other (tetraphenylporphinato)iron(III) salts with NO. With TBPH employed as a trap at 0.15 M, the yields of DA and TBP• were >99% in the case of (TPP)Fe^{III}Cl.[2c] Thus, no perceptible oxidation of DA occurs within a solvent-caged species. With (Me_8TPP)Fe^{III}Cl[2e] and $[TBPH]_i$ to 0.3 M, the asymptotic yields of DA and MA may be approximated as being about 100%, so a solvent-caged mechanism is not important. In the reaction of (Cl_8TPP)Fe^{III}Cl[2d] with NO in the presence of TBPH trap, the asymptotic yields of TBP•, DA, and MA may be approximated as 83%, 80%, and 17%, respectively. These results suggest that perhaps 20% of the oxidation of DA by (($^{+\bullet}Cl_8$TPP)Fe^{IV}O)Cl occurs within a solvent-caged intimate pair. The lack of observation of ring hydroxylation of DA when using (Cl_8TPP)Fe^{III}Cl as catalyst may be ascribed to the lower oxidation potential of ($^{+\bullet}Cl_8$TPP)Fe^{IV}O as compared to ($^{+\bullet}F_{20}$TPP)Fe^{IV}O and perhaps the greater steric hindrance of the *o*-chloro substituents which might prevent the correct orientation of the reactants as compared to the *o*-fluoro substituents.

Though our experimental results are discussed in terms of the reaction of ((F_{20}TPP)Fe^{IV}O)Cl with DA within a solvent cage (Scheme III), we have no experimental means of distinguishing this possibility from the kinetically equivalent competition between intramolecular rearrangements of the (F_{20}TPP)Fe^{III}(NO)Cl complex and oxygen transfer from N → Fe within this complex (Scheme IV). The mechanism of Scheme IV is disfavored, however, on the basis that satisfactory intramolecular concerted reactions for both dealkylation and ring hydroxylation are not obvious.

The specificity in the formation of oxidation products in the reaction of NO with substituted (tetraphenylporphinato)iron(III) salts is quite interesting. The very low yield of epoxide (based on $[NO]_i$) from *cis*-cyclooctene (~6% at 1.0 M alkene) in the presence of NO and (F_{20}TPP)Fe^{III}Cl is expected. We have previously[2e] discussed the finding that in the competition between epoxidation and DA oxidation electron withdrawing substituents on the porphyrin moiety favor amine oxidation. Both epoxidation and amine oxidation become more rapid, but amine oxidation is more sensitive to electronic effects. With (Me_8TPP)Fe^{III}Cl as catalyst in the presence of NO, the percentage yields in the epoxidation of a number of alkenes vary from 80% to 100%.[2e] When the C_2-capped (tetraphenylporphinato)iron(III) SbF_6^- salt is used, epoxidation of alkenes occurred to between 40% and 100% when $[alkene]_i$ = 1.0 M; however, at lower concentrations of alkene there were obtained in good yield tetrahydroquinolines formed by the cycloaddition of DA radical and alkene (eq 5).[2f] In the reaction

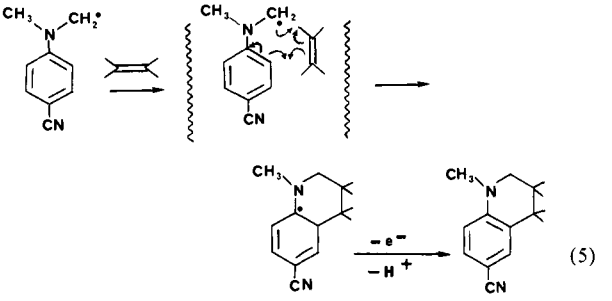

(5)

of NO with (Cl_8TPP)Fe^{III}Cl and (F_{20}TPP)Fe^{III}Cl, the amine products are DA and MA; however, with (TPP)Fe^{III}Cl and

(10) Murdoch, J. *J. Am. Chem. Soc.* **1980**, *102*, 71.

$(Me_8TPP)Fe^{III}Cl$ there is also obtained *N,N'*-dimethyl-*N,N'*-bis-(*p*-cyanophenyl)hydrazine (H) and *N,N'*-bis(*p*-cyanophenyl)-*N*-methylmethylenediamine (MD). Both H and MD

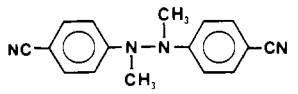

H

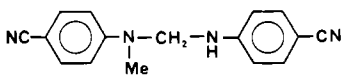

MD

would appear to arise by the coupling of radical species of MA. Apparently, with the more electron-deficient iron(IV)-oxo porphyrin π-cation radical species, DA becomes a better substrate for oxidation, sparing MA from $1e^-$ oxidation. In this study we find that the most electron-deficient iron(IV)-oxo porphyrin π-cation radical ($(^{+\bullet}F_{20}TPP)Fe^{IV}O$) is capable of hydroxylation of the aromatic ring of DA.

Acknowledgment. This work was supported by grants from the National Institutes of Health and The National Science Foundation. X-ray crystallographic studies were carried out in the Department of Chemistry and Biochemistry at UCLA by C.B.K.

Supplementary Material Available: Listing of experimental collection and reduction of X-ray data, position and vibration parameters for hydrogen, anisotropic vibration parameters for non-hydrogen atoms, position and vibration parameters for non-hydrogen atoms, bond lengths and bond angles for non-hydrogen atoms, and torsion angles (9 pages); tables of calculated and observed structure factors for 4-cyano-7-(dimethylamino)-2-benzofuranone-3-spiro-2'-cyano-5'-(dimethylamino)cyclopentadiene (9 pages). Ordering information is given on any current masthead page.

Communications to the Editor

Template and Stepwise Syntheses of a Macrobicyclic Catechoylamide Ferric Ion Sequestering Agent[1]

Thomas J. McMurry, Steven J. Rodgers,† and Kenneth N. Raymond*

Department of Chemistry, University of California Berkeley, California 94720

Received November 7, 1986

The synthesis of ligands that specifically sequester a given metal ion under physiological conditions presents a challenge to the coordination chemist.[2-7] A biomimetic approach to the synthesis of ferric ion specific chelators is suggested by the siderophores, low molecular weight sequestering agents which enable microorganisms to assimilate iron.[8] We have previously reported the synthesis of siderophore analogues with linear,[9-11] tripodal,[12,13] and macrocyclic[14] topologies,[15] some of which are promising candidates for the in vivo removal of iron as well as the actinides.[16,17] We describe here the synthesis of a new macrobicyclic catechoylamide ligand,[18] bicapped TRENCAM (**1a**), by conventional high-dilution techniques as well as the development of a high-yield template synthesis which promises to revolutionize the preparation of such ligands.

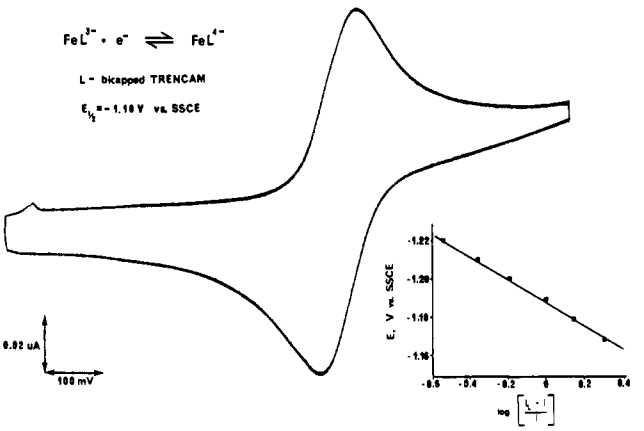

Figure 1. Cyclic voltammogram of 0.5 mM ferric(bicapped TRENCAM) in 0.4 M $NaClO_4$ (pH 12.0) at HMDE. Negative potentials (vs. SSCE) are plotted to the right and reduction currents are plotted upward. Scan rate, 50 mV/s; initial potential, -600 mV. The inset shows *E* vs. log $[(i_L - i)/i]$ for the normal pulse polarogram.

Methyl-protected bicapped TRENCAM **1b** was synthesized by two high-dilution routes (Scheme I) which resulted in cyclization yields of 3.5% and 27% after chromatography on silica gel (Chromatatron, CH_2Cl_2/5% CH_3OH). The simplicity of the ^1H and ^{13}C NMR of **1b** reflects the idealized D_{3h} symmetry of the molecule.[19] Elemental analysis and positive ion fast atom bombardment (FAB) mass spectroscopy confirmed the proposed

* Author to whom correspondence should be addressed.
† Deceased.

(1) Paper 16 in the series "Ferric Ion Sequestering Agents". Reference 34 is the previous paper in the series.
(2) *Development of Iron Chelators for Clinical Use*; Martell, A. E., Anderson, W. F., Badman, D. G., Eds.; Elsevier North-Holland: New York, 1981.
(3) May, P. M.; Bulman, R. A. *Prog. Med. Chem.* **1983**, *20*, 225-336.
(4) Edwards, G. L.; Hayes, R. R. *J. Nucl. Med.* **1969**, *10*, 103.
(5) Pecoraro, V. L.; Wong, G. B.; Raymond, K. N. *Inorg. Chem.* **1982**, *21*, 2209-2215.
(6) Moerlein, S. M.; Welch, M. J.; Raymond, K. N. *J. Nucl. Med.* **1981**, *22*, 710-719.
(7) Raymond, K. N.; Kappel.; M. J.; Pecoraro, V. L.; Harris, W. R.; Carrano, C. J.; Weitl, F. L.; Durbin, P. W. In *Actinides in Perspective*; Edelstein, N. M., Ed.; Pergamon: Oxford and New York, 1982; pp 491-507.
(8) Raymond, K. N.; Müller, G.; Matzanke, B. F. *Top. Curr. Chem.* **1984**, *123*, 50-102.
(9) Weitl, F. L.; Raymond, K. N. *J. Org. Chem.* **1981**, *46*, 5234-5237.
(10) Weitl, F. L.; Raymond, K. N. *J. Am. Chem. Soc.* **1980**, *102*, 1252-1255.
(11) Weitl, F. L.; Harris, W. R.; Raymond, K. N. *J. Med. Chem.* **1979**, *22*, 1281-1283.
(12) Weitl, F. L.; Raymond, K. N. *J. Am. Chem.* Soc. **1979**, *101*, 2728-2731.
(13) Harris, W. R.; Weitl, F. L.; Raymond, K. N. *J. Chem. Soc., Chem. Commun.* **1979**, 177-178.
(14) Rodgers, S. J.; Ng, C. Y.; Raymond, K. N. *J. Am. Chem. Soc.* **1985**, *107*, 4094-4095.
(15) Lehn, J.-M. *Science (Washington, D.C.)* **1985**, *227*, 849-856.
(16) Durbin, P. W.; Jeung, N.; Jones, E.; Weitl, F. L.; Raymond, K. N. *Radiat. Res.* **1984**, *99*, 106-128.
(17) Weitl, F. W.; Raymond, K. N.; Durbin, P. W. *J. Med. Chem.* **1981**, *26*, 439.
(18) Wolfgang, K.; Vögtle, F. *Angew. Chem., Int. Ed. Engl.* **1984**, *23*, 714.
(19) ^1H NMR (200 MHz, $CDCl_3$) δ 2.74 (br m, 12 H), 3.61 (br m, 12 H), 3.80 (s, 18 H), 6.72 (s, 6 H), 7.61 (t, 6 H, J = 4.6 Hz); ^{13}C NMR (50 MHz, $CDCl_3$) δ 36.68, 52.25, 61.57, 124.12, 131.45, 151.27, 166.28.